Current Biology 24, 1263–1270, June 2, 2014 ©2014 Elsevier Ltd All rights reserved http://dx.doi.org/10.1016/j.cub.2014.04.021

Report

Anillin Regulates Cell-Cell Junction Integrity by Organizing Junctional Accumulation of Rho-GTP and Actomyosin

Ciara C. Reyes,[1] Meiyan Jin,[2] Elaina B. Breznau,[1] Rhogelyn Espino,[2] Ricard Delgado-Gonzalo,[3] Andrew B. Goryachev,[4] and Ann L. Miller[1,2,*]

[1]The Cellular and Molecular Biology Program, University of Michigan, Ann Arbor, MI 48109, USA

[2]Department of Molecular, Cellular, and Developmental Biology, University of Michigan, Ann Arbor, MI 48109, USA

[3]Biomedical Imaging Group, École Polytechnique Fédérale de Lausanne, Lausanne 1015, Switzerland

[4]Centre for Systems Biology, School of Biological Sciences, The University of Edinburgh, Mayfield Road, Edinburgh EH9 3JR, Scotland, UK

Summary

Anillin is a scaffolding protein that organizes and stabilizes actomyosin contractile rings and was previously thought to function primarily in cytokinesis [1–10]. Using *Xenopus laevis* embryos as a model system to examine Anillin's role in the intact vertebrate epithelium, we find that a population of Anillin surprisingly localizes to epithelial cell-cell junctions throughout the cell cycle, whereas it was previously thought to be nuclear during interphase [5, 11]. Furthermore, we show that Anillin plays a critical role in regulating cell-cell junction integrity. Both tight junctions and adherens junctions are disrupted when Anillin is knocked down, leading to altered cell shape and increased intercellular spaces. Anillin interacts with Rho, F-actin, and myosin II [3, 8, 9], all of which regulate cell-cell junction structure and function. When Anillin is knocked down, active Rho (Rho-guanosine triphosphate [GTP]), F-actin, and myosin II are misregulated at junctions. Indeed, increased dynamic "flares" of Rho-GTP are observed at cell-cell junctions, whereas overall junctional F-actin and myosin II accumulation is reduced when Anillin is depleted. We propose that Anillin is required for proper Rho-GTP distribution at cell-cell junctions and for maintenance of a robust apical actomyosin belt, which is required for cell-cell junction integrity. These results reveal a novel role for Anillin in regulating epithelial cell-cell junctions.

Results and Discussion

Anillin Localizes to Cell-Cell Junctions in Epithelial Cells

The role of vertebrate Anillin has been characterized in isolated cultured cells, where it promotes stable cleavage furrow positioning during cytokinesis [3, 11–13]. Anillin is also enriched in the actomyosin-rich structures required for modified forms of cytokinesis, including cellularization and polar body emission [2, 4, 14]. However, almost nothing is known about Anillin's function during cytokinesis in vertebrate organisms in vivo, and potential roles outside cytokinesis are completely uncharacterized. Thus, we examined Anillin's localization in gastrula-stage *Xenopus laevis* embryos in which a polarized epithelium with functional cell-cell junctions has formed (Figure S1A available online) [15]. We first expressed tagged Anillin (Anillin-3XGFP) in embryos in which endogenous Anillin was depleted with a morpholino oligonucleotide (MO) (Figures 1A and S1B–S1D). Consistent with work from isolated cultured cells [2, 3, 5, 11], Anillin-3XGFP was primarily nuclear during interphase and strongly accumulated at the contractile ring during cytokinesis (Figures 1A, S1C, and S1D). Surprisingly, however, an additional population of Anillin-3XGFP was observed at cell-cell boundaries in both mitotic and interphase cells and was focused toward the apical surface (Figures 1A, S1C, and S1D; Movies S1 and S2).

Immunostaining with antibodies against *Xenopus* Anillin confirmed that endogenous Anillin localized to cell-cell junctions in both interphase and mitotic cells and was clearly focused apically at cell-cell junctions (Figures 1B, S1E, and S1F). Upon Anillin MO injection, Anillin protein levels were reduced to 42% ± 8% of control levels (Figures S1H and S1I). Anillin knockdown (KD) also led to cytokinesis defects, consistent with previous reports (Figure S1G) [3]. Furthermore, endogenous Anillin signal was sharply reduced at cell-cell junctions and in the nucleus when Anillin was knocked down, confirming that the MO targets Anillin (Figures 1B–1D). Taken together, these results demonstrate that a pool of endogenous Anillin is localized at cell-cell junctions in epithelial cells.

Anillin Is Required for Proper Adherens Junction and Tight Junction Structure

The surprising observation that Anillin localizes at cell-cell junctions led us to examine whether Anillin functionally regulates the apical junctional complex (Figure S2A). Anillin KD produced several striking junctional phenotypes. First, whereas the apical cell membranes were closely apposed in control cells, Anillin-depleted cells often exhibited intercellular spaces (Figure 2A). Second, control cells were polygonal and came to a point at tricellular junctions (the sites where three cells come together), but Anillin KD cells exhibited a rounded shape (Figure 2A), suggesting that Anillin may be important for junctional tension. Third, β-catenin, an adherens junction (AJ) plaque protein, was apically enriched at the zonula adherens in controls (Figures 2B and 2F). However, in Anillin KD embryos, basolateral localization of β-catenin was retained, but the increased apical concentration was lost (Figures 2B and 2F). Importantly, when Anillin mRNA was re-expressed in cells where endogenous Anillin was depleted, the effect on β-catenin was partially rescued (Figures S2B and S2C). Fourth, when Anillin was depleted, staining for E-Cadherin, an AJ transmembrane protein, showed strongly reduced signal and reduced apical concentration (Figure 2C).

To determine whether Anillin likewise participates in tight junction (TJ) structure, the TJ proteins ZO-1 and Claudin were analyzed. In control cells, staining for the TJ plaque protein ZO-1 was sharp and linear at cell-cell junctions, present at the apical surface of each cell-cell junction, and enriched at tricellular TJs relative to bicellular TJs (Figures 2D and S2D). In contrast, in Anillin KD cells, ZO-1 accumulation was discontinuous and wavy (Figures 2D and S2D), suggesting that Anillin depletion may result in decreased apicolateral

*Correspondence: annlm@umich.edu

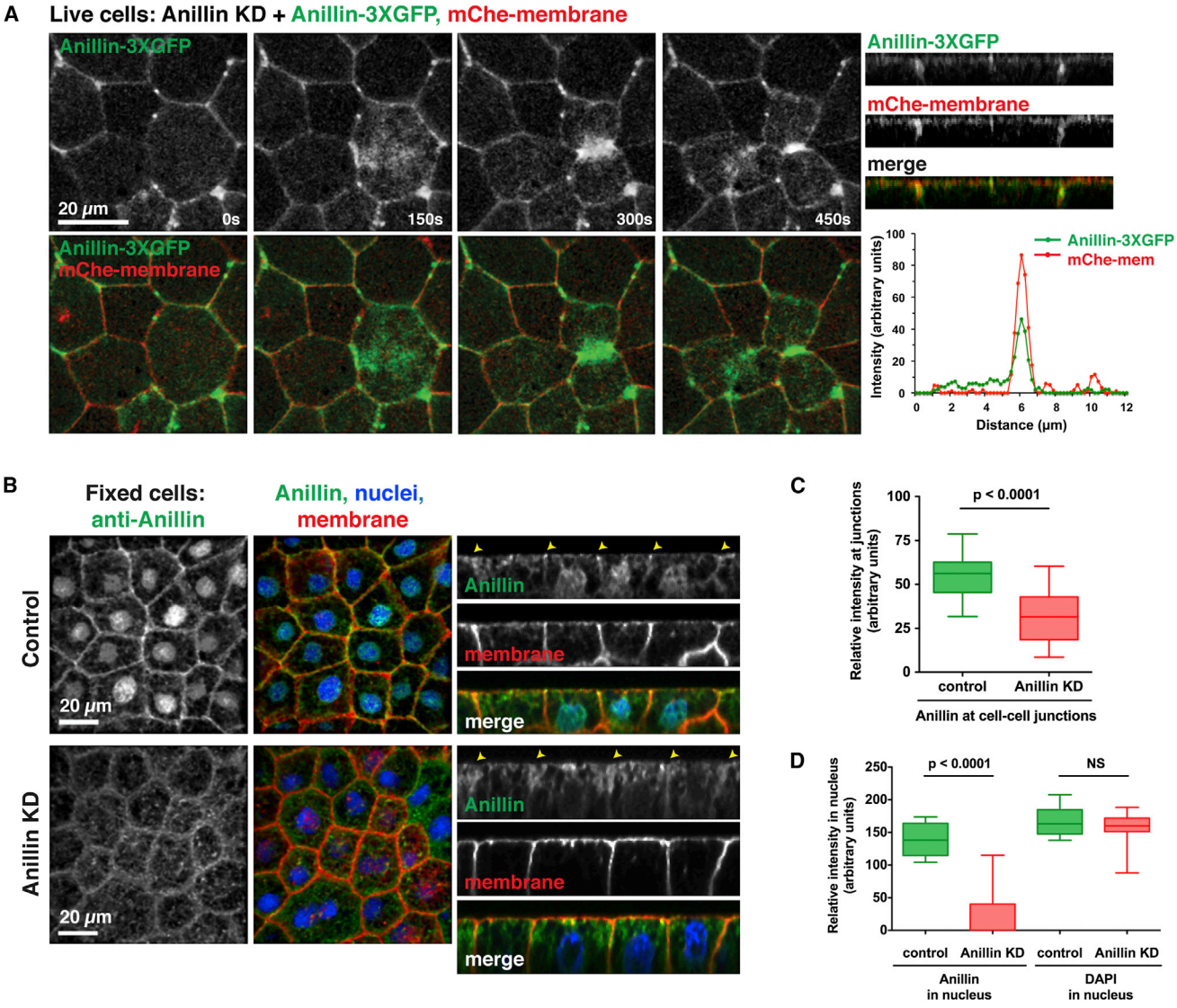

Figure 1. Anillin Localizes at Cell-Cell Junctions in Interphase and Mitotic Epithelial Cells

(A) Live imaging of Anillin-3XGFP in gastrula-stage embryos in which endogenous Anillin was depleted. mCherry-membrane labels the plasma membrane. Images are brightest point projections of 17 apical z planes. Nuclear Anillin is not visible because only apical planes were captured. Right: z view shows that Anillin-3XGFP is apically focused. Graph shows an average of five line scans drawn perpendicular to junctions, indicating that the peak intensities of Anillin-3XGFP and mCherry-membrane overlap.

(B) Embryos were injected with a GFP-membrane injection marker with or without the Anillin MO. Gastrula-stage embryos were fixed and stained with an anti-Anillin antibody (pseudocolored green), anti-GFP to view the membrane (pseudocolored red), and DAPI (blue). z views show that apically focused Anillin accumulation at cell-cell junctions is reduced when Anillin is depleted (yellow arrowheads).

(C) Quantification of the average intensity of endogenous Anillin at cell-cell junctions in control and Anillin KD cells (see Supplemental Experimental Procedures for details). Data are from three separate experiments; n = 18 embryos for control and n = 19 embryos for Anillin KD, graphed as box-and-whisker plot with the whiskers representing the 1st–99th percentile; $p < 0.0001$.

(D) Quantification of the average endogenous Anillin and DAPI intensity in the nucleus in control and Anillin KD cells (see Supplemental Experimental Procedures for details). Data are from three independent experiments; n = 18 embryos for control and n = 19 embryos for Anillin KD, graphed as box-and-whisker plot with the whiskers representing the 1st–99th percentile; $p < 0.0001$ for control versus Anillin KD for nuclear Anillin signal; $p = 0.16$ for control versus Anillin KD for DAPI signal.

See also Figure S1 and Movies S1 and S2.

tension [16]. In Anillin KD cells, concentrated ZO-1 was not observed at the apical surface of each cell-cell junction and was sometimes buried basally (Figure 2D). Additionally, ZO-1 was not strongly enriched at tricellular TJs in Anillin KD cells (Figure S2D). Staining for Claudin, a TJ transmembrane protein, showed that the relative intensity of Claudin at TJs was significantly decreased in Anillin KD embryos (Figures 2E and 2G). Taken together, these findings demonstrate that Anillin is required for proper organization of both AJ and TJ structure in epithelial cells.

Anillin Is Required for Junctional Integrity

Because the apical junctional complex forms adhesive contacts between cells and limits the passage of molecules across

the epithelium, we tested how the defects in AJs and TJs in Anillin KD embryos affect passage of a low-molecular-weight (3 kDa) fluorescent dextran between cells (Figure S2E) [15, 17]. In control embryos, dextran was restricted above the surface of the epithelium; however, in Anillin KD embryos, dextran penetrated into intercellular spaces around the perimeter of the cells, particularly at tricellular junctions (Figure 3A). A similar increase in dextran penetration was observed in embryos treated with EGTA to disrupt junctions by depleting calcium (Figure S2F) [18, 19]. Both the average percentage of junctions breached by dextran and the average depth of dextran penetration into the intercellular spaces were significantly increased in Anillin-depleted embryos (Figures 3B and 3C). The increased dextran penetration in Anillin KD embryos likely reflects both increased permeability, as we observed cases in which the 3 kDa fluorescent dextran penetrated deeply between the cells as a thread-like protrusion (Figure S2G), and the apically domed cell shape observed in Anillin KD embryos (see z views of Anillin KD cells in Figures 1, 2, and 3). Taken together, these results suggest that junctional integrity is compromised when Anillin is depleted.

Anillin Is Necessary for Proper Distribution of Rho-GTP at Cell-Cell Junctions

We next examined the mechanism by which Anillin regulates cell-cell junctions. The interaction between Anillin and Rho involves a positive feedback loop: Anillin's localization to the cleavage furrow is dependent on active Rho [3, 8, 20], and Anillin, in turn, promotes active Rho accumulation and stability at the cleavage furrow [8, 21]. Therefore, we reasoned that junctional Rho activity might be altered when Anillin is perturbed. Using a fluorescent probe that binds specifically to Rho-guanosine triphosphate (GTP) (GFP-Rho-binding domain of Rhotekin [rGBD]) [22], we observed that in control cells, Rho-GTP was present at cell-cell junctions and at the cleavage furrow throughout cytokinesis (Figures S3A and S3C; Movie S3). Additionally, dividing cells pulled neighboring cells along with the constricting cleavage furrow (Figure S3B). In contrast, active Rho was not restricted to the cleavage furrow during cytokinesis in Anillin KD embryos. Instead, intense "flares" of active Rho appeared at ectopic positions around the perimeter of the dividing cell, as well as in neighboring cells (Figures S3A and S3C; Movie S3), indicating that tension asymmetries in Anillin KD cells may be mechanically integrated among multiple cells [23, 24]. Furthermore, junctions were often not properly maintained during cell division in Anillin KD embryos, and the dividing cell separated from its neighboring cells (Figure S3B).

Because Anillin depletion disrupted cell-cell junctions in both dividing and nondividing cells, we examined the effect of Anillin KD on active Rho localization at junctions in nondividing regions of the epithelium. In control cells, occasional fluctuations in junctional Rho-GTP were observed (Figure 4A and Movie S4); however, in Anillin KD cells, a pronounced increase in flares of Rho-GTP was observed around cell-cell junctions, particularly at tricellular junctions (Figure 4A and Movie S4). Kymographs generated from time-lapse movies allowed us to quantify the frequency, lifetime, intensity, and breadth of the Rho-GTP flares over time (Figures 4B and S3D), revealing a statistically significant increase in the frequency and a reduction in the lifetime of Rho-GTP flares when Anillin is knocked down (Figures 4C and 4D). Although a significant change in Rho-GTP flare intensity was not observed (data not shown), the breadth of flares was increased in Anillin KD embryos (Figure 4E). Notably, the Rho-GTP flares were rapidly followed by strong F-actin accumulation (Figure 4B), indicating that Rho-GTP flares may be sites of local mechanical perturbation in the epithelia. Together, these results suggest that Anillin is important for proper distribution of junctional Rho-GTP in both mitotic and interphase cells.

Anillin Scaffolds the Apical Actomyosin Belt in Epithelial Cells

Rho signaling can drive junction assembly and disassembly by regulating the tension in the apical actomyosin belt that connects to AJs and TJs (Figure S2A) [25, 26]. Because Anillin is required for proper accumulation of Rho-GTP at junctions (Figures 4A–4E), and Anillin can bind directly to F-actin and myosin II [2, 3], we hypothesized that loss of proper apical junctional structure and function in Anillin KD embryos could be due to disruption of the apical actomyosin belt. To test this idea, we first stained control, Anillin KD, and Anillin-overexpressing (OE) embryos for F-actin. F-actin accumulated in a strong apical band in controls, but Anillin depletion decreased the intensity and breadth of F-actin accumulation at cell-cell junctions (Figures 4F, 4H, and S3F). Moreover, Anillin OE increased the intensity of F-actin at cell-cell junctions and led to intense, spiky contractile rings in dividing cells (Figures 4F, S3E, and S3F; Movie S5), suggesting that Anillin is hyperactive in its role as a scaffolding protein when OE.

Phosphorylation of the regulatory light chain of myosin II (P-MLC) promotes the adenosine triphosphatase activity of myosin II, which is necessary for generating actomyosin contraction [27]. Therefore, increased P-MLC staining can be used as a readout for increased tension. In control embryos, P-MLC was localized along bicellular junctions and was intensely localized at tricellular junctions (Figure 4G); however, P-MLC intensity was significantly reduced in Anillin KD embryos (Figures 4G and 4I). Furthermore, when Anillin was OE, P-MLC accumulated strongly at junctions and at the apical cell cortex, and cells appeared hypercontractile (Figures 4G and S3G). These results support the idea that Anillin scaffolds the apical actomyosin belt. We propose that Anillin is necessary to stabilize and properly distribute tension in the apical actomyosin belt (Figure 4J).

Conclusions

Our results demonstrate that Anillin, which was previously thought to be nuclear during interphase and function solely in cytokinesis [11, 12], plays a critical role in interphase and dividing epithelial cells, where it regulates cell-cell junctions. Whereas previous research on Anillin was generally conducted in isolated cells, our work in an intact vertebrate epithelium revealed this novel function for Anillin. Clues to Anillin's localization at junctions were observed previously, including the cortical localization of Anillin in blastula-stage *Xenopus* embryos [28] and the apparent localization of Anillin to junctions in interphase epithelial cells of gastrulating *Drosophila* embryos [2]. However, other studies in the *Drosophila* epithelia did not reveal junctional localization for Anillin [29]. We show here that a pool of Anillin localizes to cell-cell junctions in interphase and mitotic cells and regulates apical junctional structure and function in epithelial cells of the gastrulating *Xenopus* embryo. We predict that Anillin's role in regulating cell-cell junctions is likely conserved among higher vertebrates because Anillin and the other key players are highly conserved.

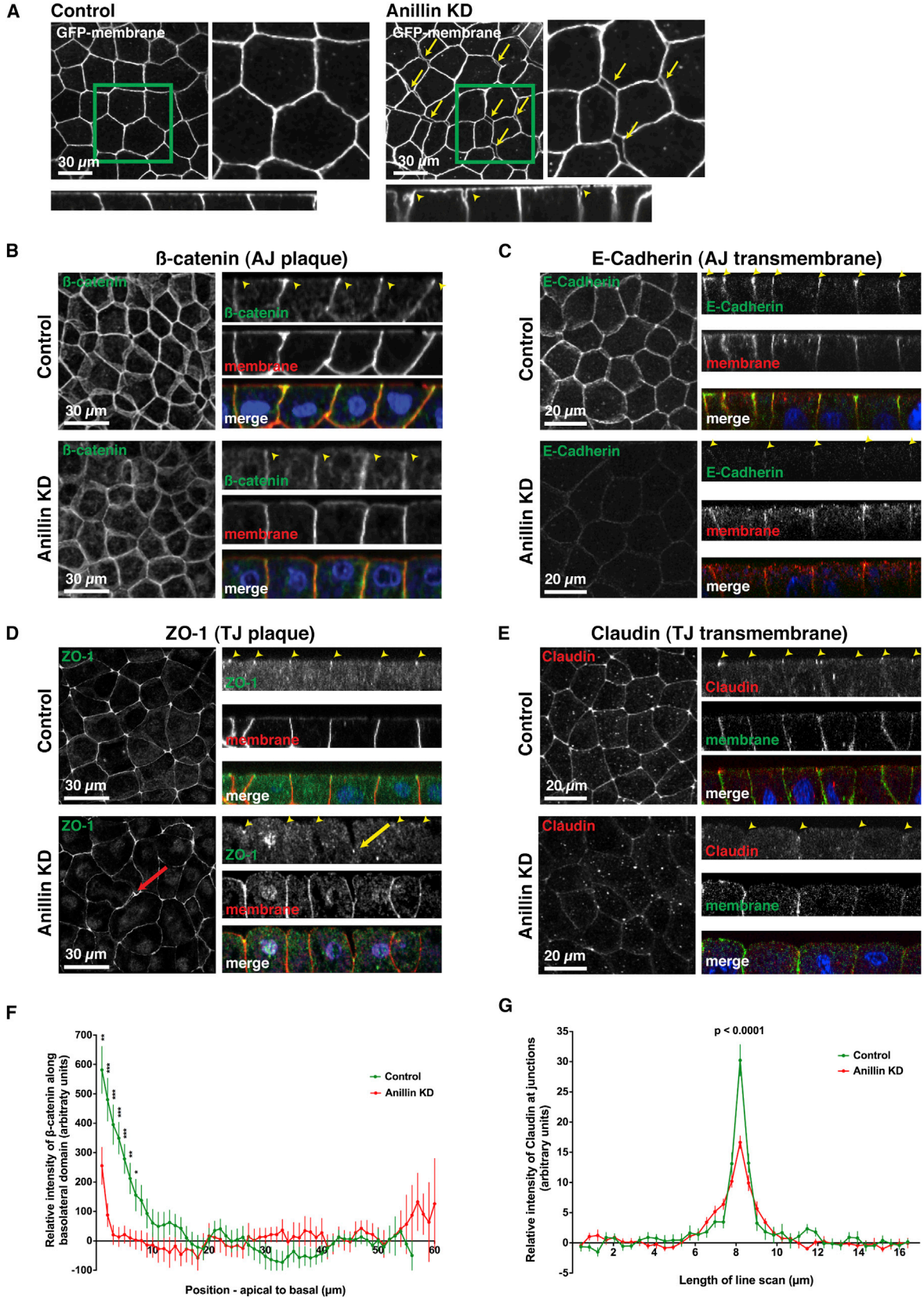

Figure 2. AJs and TJs Are Disrupted when Anillin Is Knocked Down

(A) Single intermediate plane views (top) and z views (bottom) of GFP-membrane in control and Anillin KD embryos reveal increased intercellular spaces in Anillin KD embryos (yellow arrows and arrowheads).

(legend continued on next page)

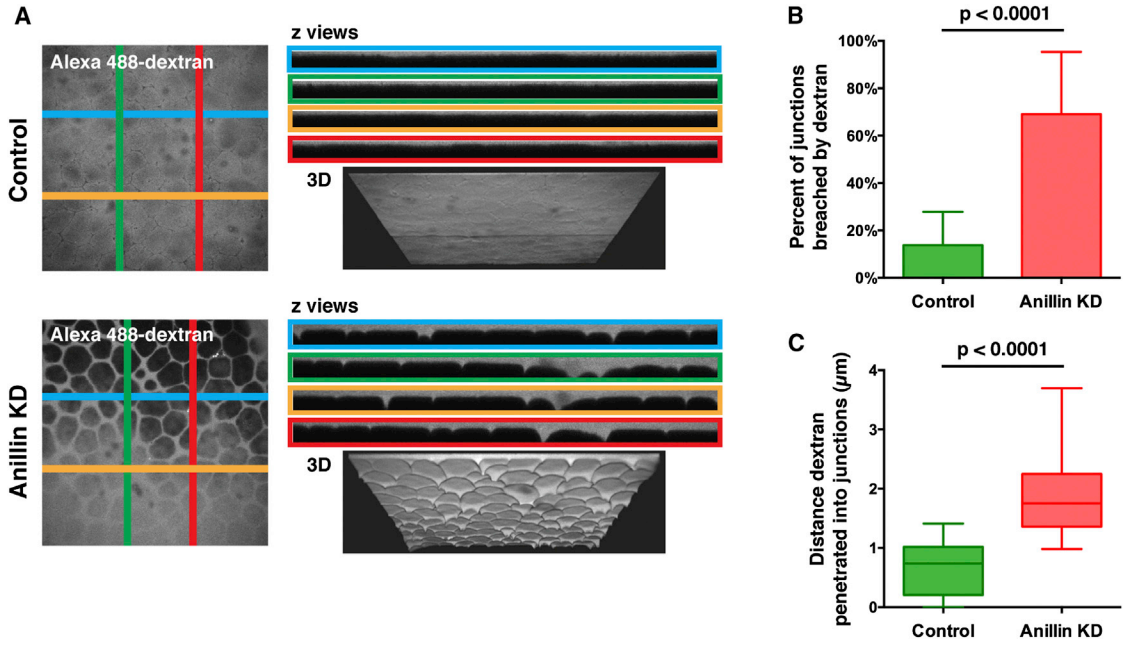

Figure 3. Junctional Integrity Is Compromised when Anillin Is Knocked Down

(A) Live control or Anillin KD embryos were mounted in 3,000 molecular weight (MW) Alexa 488-Dextran. Left: x-y views show that dextran can penetrate between rounded cells in Anillin KD embryos. Right: z views generated along the indicated lines (top) and 3D views (bottom) show that, although dextran remains at the surface in control embryos, it can penetrate between cells in Anillin KD embryos.

(B) Quantification of the average percentage of junctions where dextran penetrated into the intercellular space in control and Anillin KD embryos. Data are from three independent experiments; n = 13 embryos for controls and n = 17 embryos for Anillin KD, graphed as mean + SEM; $p < 0.0001$.

(C) Quantification of the average depth of dextran penetration for control and Anillin KD embryos. Data are from three independent experiments; n = 13 embryos for controls and n = 17 embryos for Anillin KD, graphed as box-and-whisker plot with the whiskers representing the 1st–99th percentile; $p < 0.0001$. See also Figure S2.

The defects reported in AJ and TJ structure in Anillin-depleted cells were observed in both dividing and nondividing cells. Importantly, these defects were observed in mononucleate cells, demonstrating that the effects on cell-cell junctions are not secondary to the cytokinesis defect. We have not yet examined how cell division failure elsewhere in the epithelium may perturb tension homeostasis or affect cell-cell junctions at a distance, but this will be an interesting question for future studies.

We propose that Anillin regulates cell-cell junction integrity by controlling the distribution of junctional Rho-GTP and stabilizing the apical actomyosin belt (Figure 4J). We show that Anillin is required for proper distribution of Rho-GTP at apical junctions. Our live imaging of junctional Rho-GTP dynamics extends previous fixed-imaging studies showing that a localized zone of Rho-GTP forms at cell-cell junctions [26, 30–32]. We show that when Anillin is depleted, the sustained junctional Rho activation observed in controls is replaced by frequent, dynamic flares of Rho-GTP followed rapidly by increased F-actin accumulation. We propose that the pronounced Rho-GTP flares in Anillin KD embryos may represent sites of junction disassembly or repair. Although the mechanisms that control localized formation and dynamics of the junctional Rho-GTP zone are not well understood, emerging evidence implicates a number of proteins known to regulate Rho activity during cytokinesis, including MgcRacGAP, Ect2, p190RhoGAP, and GEF-H1 [17, 30, 33, 34]. Interestingly, Anillin binds MgcRacGAP [6, 7] and Ect2 [10] and could serve as a scaffold to recruit and/or retain them at cell-cell junctions. Thus, Anillin may be involved in regulating the distribution of junctional Rho-GTP directly through its ability to bind Rho or indirectly through its

(B–E) Fixed staining of control and Anillin KD embryos for β-catenin (B), E-Cadherin (C), ZO-1 (D), and Claudin (E). GFP-membrane or mChe-membrane was used as a MO injection marker, and DAPI labels DNA. z views show the normal localization of the cell-cell junction proteins in control cells as well as the disrupted localization in Anillin KD cells (see yellow arrowheads). The x-y TJ protein images on the left in (D) and (E) are maximal-intensity projections of serial z sections. The red arrow in (D) highlights an intercellular space between a dividing cell and its neighbor, whereas the yellow arrow indicates a ZO-1 concentration that is buried basally.

(F) Quantification of β-catenin polarization in control and Anillin KD cells from line scans along the basolateral surface. The β-catenin signal at the ten most-basal points was normalized to zero so that data from multiple embryos could be averaged (see Supplemental Experimental Procedures for details). Data are from two independent experiments; n = 26 embryos for control and n = 18 embryos for Anillin KD, graphed as mean ± SEM; *$p \leq 0.05$, **$p \leq 0.01$, ***$p \leq 0.001$.

(G) Quantification of the relative intensity of Claudin at cell-cell junctions by generating line scans perpendicular to junctions (see Supplemental Experimental Procedures for details). Data are from two independent experiments; n = 10 embryos for control and n = 12 for Anillin KD, graphed as mean ± SEM; $p < 0.0001$.

See also Figure S2.

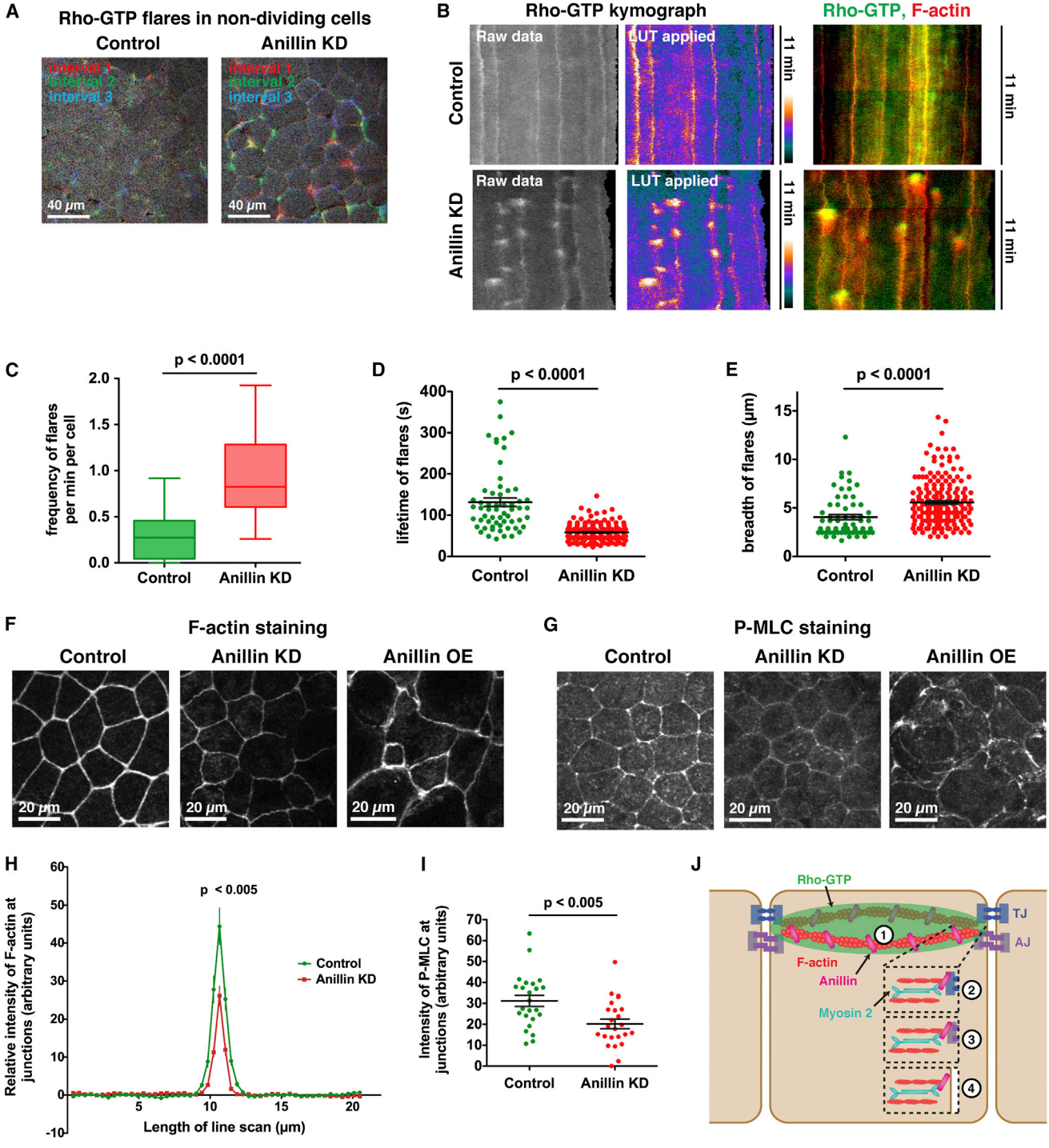

Figure 4. Anillin Regulates the Distribution of Rho-GTP, F-Actin, and Phospho-Myosin II at Cell-Cell Junctions

(A) Embryos were injected with GFP-rGBD (Rho-binding domain of Rhotekin) as a probe for active Rho. Brightest point projections of Rho-GTP flares over three time intervals in nondividing control and Anillin KD cells (see Supplemental Experimental Procedures). Red indicates flare during minutes 0–2.5; green indicates flare during minutes 2.5–5; blue indicates flare during minutes 5–7.5; white indicates overlap of Rho-GTP flares.

(B) Rho-GTP kymographs for nondividing control and Anillin KD cells. Left: raw data and LUT kymographs (see Supplemental Experimental Procedures) show increased Rho-GTP flares in Anillin KD cells, which occur more frequently along tricellular junctions (vertical lines in kymographs). Right: kymographs with Rho-GTP (green) and F-actin (red) overlaid.

(C) Quantification of frequency of Rho-GTP flares per minute per cell for control and Anillin KD embryos. Data are from three independent experiments; n = 21 kymographs for controls and n = 21 kymographs for Anillin KD, graphed as box-and-whisker plot with the whiskers representing the 1st–99th percentile; $p < 0.0001$.

(D) Quantification of the lifetime of Rho-GTP flares for control and Anillin KD embryos. Data are from two independent experiments; n = 59 flares from 16 kymographs for controls and n = 177 flares from 16 kymographs for Anillin KD, graphed as a scatter dot plot with mean ± SEM indicated; $p < 0.0001$.

(legend continued on next page)

interactions with Ect2 and MgcRacGAP. Additionally, Ect2 can regulate function of the Par6/Par3/PKCζ polarity complex through Cdc42, thus playing a role in epithelial junction assembly and cell polarity [33]; therefore, it would be interesting to test whether Anillin depletion also affects Cdc42 activation at cell-cell junctions.

Anillin is a strong candidate to scaffold and organize the apical actomyosin belt at cell-cell junctions, given its interactions with F-actin, myosin II, and the formin mDia2 [2, 3, 9, 35]. We show here that Anillin regulates the proper accumulation of F-actin and P-MLC at cell-cell junctions. The cell rounding and apical doming phenotypes observed when Anillin is perturbed likely result from changes in tension of the apical actomyosin belt because apical doming has been observed in other situations in which apical tension is altered [36, 37]. Our data suggest that Anillin is required for properly distributing Rho-GTP and scaffolding the apical actomyosin belt (Figure 4J). However, Anillin could potentially make direct connections with a TJ and/or AJ component or use its pleckstrin homology domain to directly couple the apical actomyosin belt to the plasma membrane (Figure 4J); these will be important avenues for future research. Finally, Anillin is OE 2- to 6-fold in diverse human tumors, and higher expression levels correlate with increased metastatic potential [38, 39]. Therefore, misregulation of cell-cell junctions represents a novel mechanism by which Anillin may contribute to cancer progression.

Supplemental Information

Supplemental Information includes Supplemental Experimental Procedures, three figures, and five movies and can be found with this article online at http://dx.doi.org/10.1016/j.cub.2014.04.021.

Acknowledgments

All studies with *Xenopus laevis* embryos were conducted in compliance with the US Department of Health and Human Services Guide for the Care and Use of Laboratory Animals and were approved by the University Committee on Use and Care of Animals at the University of Michigan. We thank Aaron Straight for the *Xenopus* Anillin construct and antibody; Zsuzsanna Püspöki, Virginie Uhlmann, and Michael Unser for their respective contributions to the development of Kymographer and other members of the Biomedical Imaging Group, EPFL, for helpful discussions; Sarah Woolner and Jean-Pierre Tassan for staining advice; Megan Fekete for excellent technical support; Billie Weber for making mChe-farnesyl; and members of the A.L.M. laboratory for helpful input and critical reading of the manuscript. We give special thanks to William Bement for advice, encouragement, and useful feedback. This work was supported by a grant from the NIH (R00 GM089765) to A.L.M. C.C.R. and E.B.B. were supported by the NSF Predoctoral Fellowship and the NIH Cellular and Molecular Biology Training Grant (T32-GM007315).

Received: August 20, 2013
Revised: February 24, 2014
Accepted: April 9, 2014
Published: May 15, 2014

References

1. Liu, J., Fairn, G.D., Ceccarelli, D.F., Sicheri, F., and Wilde, A. (2012). Cleavage furrow organization requires PIP(2)-mediated recruitment of anillin. Curr. Biol. *22*, 64–69.
2. Field, C.M., and Alberts, B.M. (1995). Anillin, a contractile ring protein that cycles from the nucleus to the cell cortex. J. Cell Biol. *131*, 165–178.
3. Straight, A.F., Field, C.M., and Mitchison, T.J. (2005). Anillin binds nonmuscle myosin II and regulates the contractile ring. Mol. Biol. Cell *16*, 193–201.
4. Field, C.M., Coughlin, M., Doberstein, S., Marty, T., and Sullivan, W. (2005). Characterization of anillin mutants reveals essential roles in septin localization and plasma membrane integrity. Development *132*, 2849–2860.
5. Oegema, K., Savoian, M.S., Mitchison, T.J., and Field, C.M. (2000). Functional analysis of a human homologue of the Drosophila actin binding protein anillin suggests a role in cytokinesis. J. Cell Biol. *150*, 539–552.
6. D'Avino, P.P., Takeda, T., Capalbo, L., Zhang, W., Lilley, K.S., Laue, E.D., and Glover, D.M. (2008). Interaction between Anillin and RacGAP50C connects the actomyosin contractile ring with spindle microtubules at the cell division site. J. Cell Sci. *121*, 1151–1158.
7. Gregory, S.L., Ebrahimi, S., Milverton, J., Jones, W.M., Bejsovec, A., and Saint, R. (2008). Cell division requires a direct link between microtubule-bound RacGAP and Anillin in the contractile ring. Curr. Biol. *18*, 25–29.
8. Piekny, A.J., and Glotzer, M. (2008). Anillin is a scaffold protein that links RhoA, actin, and myosin during cytokinesis. Curr. Biol. *18*, 30–36.
9. Miller, K.G., and Alberts, B.M. (1989). F-actin affinity chromatography: technique for isolating previously unidentified actin-binding proteins. Proc. Natl. Acad. Sci. USA *86*, 4808–4812.
10. Frenette, P., Haines, E., Loloyan, M., Kinal, M., Pakarian, P., and Piekny, A. (2012). An anillin-Ect2 complex stabilizes central spindle microtubules at the cortex during cytokinesis. PLoS ONE *7*, e34888.
11. D'Avino, P.P. (2009). How to scaffold the contractile ring for a safe cytokinesis - lessons from Anillin-related proteins. J. Cell Sci. *122*, 1071–1079.
12. Piekny, A.J., and Maddox, A.S. (2010). The myriad roles of Anillin during cytokinesis. Semin. Cell Dev. Biol. *21*, 881–891.
13. Goldbach, P., Wong, R., Beise, N., Sarpal, R., Trimble, W.S., and Brill, J.A. (2010). Stabilization of the actomyosin ring enables spermatocyte cytokinesis in Drosophila. Mol. Biol. Cell *21*, 1482–1493.
14. Dorn, J.F., Zhang, L., Paradis, V., Edoh-Bedi, D., Jusu, S., Maddox, P.S., and Maddox, A.S. (2010). Actomyosin tube formation in polar body cytokinesis requires Anillin in C. elegans. Curr. Biol. *20*, 2046–2051.
15. Merzdorf, C.S., Chen, Y.H., and Goodenough, D.A. (1998). Formation of functional tight junctions in Xenopus embryos. Dev. Biol. *195*, 187–203.
16. Smutny, M., Cox, H.L., Leerberg, J.M., Kovacs, E.M., Conti, M.A., Ferguson, C., Hamilton, N.A., Parton, R.G., Adelstein, R.S., and Yap, A.S. (2010). Myosin II isoforms identify distinct functional modules that support integrity of the epithelial zonula adherens. Nat. Cell Biol. *12*, 696–702.

(E) Quantification of breadth of Rho-GTP flares for control and Anillin KD embryos. Data are from two independent experiments; n = 62 flares from 16 kymographs for controls and n = 190 flares from 16 kymographs for Anillin KD, graphed as a scatter dot plot with mean ± SEM indicated; $p < 0.0001$.
(F) Fixed staining for F-actin in control, Anillin KD, and Anillin OE embryos. In Anillin KD embryos, junctional accumulation of F-actin is reduced, whereas in Anillin OE embryos, it is more intense at cell-cell junctions and the cell cortex, and cell shapes are abnormal.
(G) Fixed staining for P-MLC in control, Anillin KD, and Anillin OE embryos. In Anillin KD embryos, junctional accumulation of P-MLC is reduced, whereas in Anillin OE embryos, P-MLC is strongly accumulated at junctions and the cell cortex.
(H) Quantification of the relative intensity of F-actin at cell-cell junctions. Line scans from control and Anillin KD embryos were acquired and normalized (see Supplemental Experimental Procedures). Data are from three independent experiments; n = 24 embryos for control and n = 23 embryos for Anillin KD, graphed as mean ± SEM; $p < 0.005$.
(I) Quantification of the intensity of P-MLC at cell-cell junctions. Data are from four independent experiments; n = 24 embryos for control and n = 24 embryos for Anillin KD, graphed as a scatter dot plot with mean ± SEM indicated; $p < 0.005$.
(J) Model showing possible mechanisms by which Anillin may regulate cell-cell junctions. Although our results suggest that Anillin regulates cell-cell junction integrity by controlling the distribution of junctional Rho-GTP and stabilizing the apical actomyosin belt (1), it is also possible that Anillin may directly interact with a TJ component (2) or an AJ component (3) or link the apical actomyosin belt with the plasma membrane (4).
See also Figure S3 and Movies S3, S4, and S5.

17. Benais-Pont, G., Punn, A., Flores-Maldonado, C., Eckert, J., Raposo, G., Fleming, T.P., Cereijido, M., Balda, M.S., and Matter, K. (2003). Identification of a tight junction-associated guanine nucleotide exchange factor that activates Rho and regulates paracellular permeability. J. Cell Biol. *160*, 729–740.
18. Liu, K.C., and Cheney, R.E. (2012). Myosins in cell junctions. BioArchitecture *2*, 158–170.
19. Palmer, J.F., and Slack, C. (1970). Some bio-electric parameters of early Xenopus embryos. J. Embryol. Exp. Morphol. *24*, 535–553.
20. Hickson, G.R., and O'Farrell, P.H. (2008). Rho-dependent control of anillin behavior during cytokinesis. J. Cell Biol. *180*, 285–294.
21. Zhao, W.M., and Fang, G. (2005). Anillin is a substrate of anaphase-promoting complex/cyclosome (APC/C) that controls spatial contractility of myosin during late cytokinesis. J. Biol. Chem. *280*, 33516–33524.
22. Benink, H.A., and Bement, W.M. (2005). Concentric zones of active RhoA and Cdc42 around single cell wounds. J. Cell Biol. *168*, 429–439.
23. Fernandez-Gonzalez, R., Simoes, Sde.M., Röper, J.C., Eaton, S., and Zallen, J.A. (2009). Myosin II dynamics are regulated by tension in intercalating cells. Dev. Cell *17*, 736–743.
24. Clark, A.G., Miller, A.L., Vaughan, E., Yu, H.Y., Penkert, R., and Bement, W.M. (2009). Integration of single and multicellular wound responses. Curr. Biol. *19*, 1389–1395.
25. Rodgers, L.S., and Fanning, A.S. (2011). Regulation of epithelial permeability by the actin cytoskeleton. Cytoskeleton (Hoboken) *68*, 653–660.
26. Terry, S., Nie, M., Matter, K., and Balda, M.S. (2010). Rho signaling and tight junction functions. Physiology (Bethesda) *25*, 16–26.
27. Vicente-Manzanares, M., Ma, X., Adelstein, R.S., and Horwitz, A.R. (2009). Non-muscle myosin II takes centre stage in cell adhesion and migration. Nat. Rev. Mol. Cell Biol. *10*, 778–790.
28. Le Page, Y., Chartrain, I., Badouel, C., and Tassan, J.P. (2011). A functional analysis of MELK in cell division reveals a transition in the mode of cytokinesis during Xenopus development. J. Cell Sci. *124*, 958–968.
29. Haglund, K., Nezis, I.P., Lemus, D., Grabbe, C., Wesche, J., Liestøl, K., Dikic, I., Palmer, R., and Stenmark, H. (2010). Cindr interacts with anillin to control cytokinesis in Drosophila melanogaster. Curr. Biol. *20*, 944–950.
30. Ratheesh, A., Gomez, G.A., Priya, R., Verma, S., Kovacs, E.M., Jiang, K., Brown, N.H., Akhmanova, A., Stehbens, S.J., and Yap, A.S. (2012). Centralspindlin and α-catenin regulate Rho signalling at the epithelial zonula adherens. Nat. Cell Biol. *14*, 818–828.
31. Ratheesh, A., and Yap, A.S. (2012). A bigger picture: classical cadherins and the dynamic actin cytoskeleton. Nat. Rev. Mol. Cell Biol. *13*, 673–679.
32. Terry, S.J., Zihni, C., Elbediwy, A., Vitiello, E., Leefa Chong San, I.V., Balda, M.S., and Matter, K. (2011). Spatially restricted activation of RhoA signalling at epithelial junctions by p114RhoGEF drives junction formation and morphogenesis. Nat. Cell Biol. *13*, 159–166.
33. Liu, X.F., Ishida, H., Raziuddin, R., and Miki, T. (2004). Nucleotide exchange factor ECT2 interacts with the polarity protein complex Par6/Par3/protein kinase Czeta (PKCzeta) and regulates PKCzeta activity. Mol. Cell. Biol. *24*, 6665–6675.
34. Wildenberg, G.A., Dohn, M.R., Carnahan, R.H., Davis, M.A., Lobdell, N.A., Settleman, J., and Reynolds, A.B. (2006). p120-catenin and p190RhoGAP regulate cell-cell adhesion by coordinating antagonism between Rac and Rho. Cell *127*, 1027–1039.
35. Watanabe, S., Okawa, K., Miki, T., Sakamoto, S., Morinaga, T., Segawa, K., Arakawa, T., Kinoshita, M., Ishizaki, T., and Narumiya, S. (2010). Rho and anillin-dependent control of mDia2 localization and function in cytokinesis. Mol. Biol. Cell *21*, 3193–3204.
36. Fanning, A.S., Van Itallie, C.M., and Anderson, J.M. (2012). Zonula occludens-1 and -2 regulate apical cell structure and the zonula adherens cytoskeleton in polarized epithelia. Mol. Biol. Cell *23*, 577–590.
37. Yonemura, S., Wada, Y., Watanabe, T., Nagafuchi, A., and Shibata, M. (2010). alpha-Catenin as a tension transducer that induces adherens junction development. Nat. Cell Biol. *12*, 533–542.
38. Hall, P.A., Todd, C.B., Hyland, P.L., McDade, S.S., Grabsch, H., Dattani, M., Hillan, K.J., and Russell, S.E. (2005). The septin-binding protein anillin is overexpressed in diverse human tumors. Clin. Cancer Res. *11*, 6780–6786.
39. Suzuki, C., Daigo, Y., Ishikawa, N., Kato, T., Hayama, S., Ito, T., Tsuchiya, E., and Nakamura, Y. (2005). ANLN plays a critical role in human lung carcinogenesis through the activation of RHOA and by involvement in the phosphoinositide 3-kinase/AKT pathway. Cancer Res. *65*, 11314–11325.